ACS central science

Research Article

http://pubs.acs.org/journal/acscii

Molecular Caging of Graphene with Cyclohexane: Transfer and Electrical Transport

Liubov A. Belyaeva, Wangyang Fu, Hadi Arjmandi-Tash, and Grégory F. Schneider*

Faculty of Science, Leiden Institute of Chemistry, Leiden University, Einsteinweg 55, 2333CC Leiden, The Netherlands

ABSTRACT: Transfer of large, clean, crack- and fold-free graphene sheets is a critical challenge in the field of graphene-based electronic devices. Polymers, conventionally used for transferring two-dimensional materials, irreversibly adsorb yielding a range of unwanted chemical functions and contaminations on the surface. An oil−water interface represents an ideal support for graphene. Cyclohexane, the oil phase, protects graphene from mechanical deformation and minimizes vibrations of the water surface. Remarkably, cyclohexane solidifies at 7 °C forming a plastic crystal phase molecularly conforming graphene, preventing the use of polymers, and thus drastically limiting contamination. Graphene floating at the cyclohexane/water interface exhibits improved electrical performances allowing for new possibilities of in situ, flexible sensor devices at a water interface.

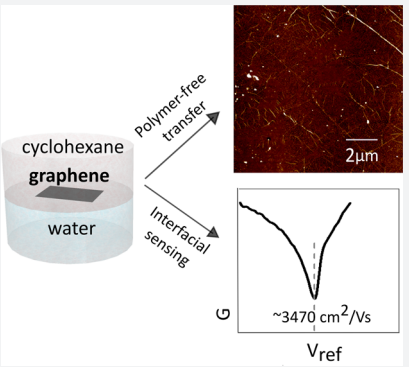

For years now, long chain polymers have been used to prevent cracking and to preserve the two-dimensional nature of graphene[1] grown by chemical vapor deposition (CVD) during transfer.[2−6] Because of their macromolecular structures, polymers can hardly be removed from the graphene surface:[7−9] they irreversibly adsorb and modify the chemical and physical properties of graphene.[10,11] Instead of using polymers, so-called polymer-free transfer techniques use special frames and holders to keep the sheet integrity of graphene.[12,13] Very recently, a biphasic system composed of an aqueous solution of ammonium persulfate and hexane has been employed for clean graphene transfer.[14] Polymer-free transfers, however, are widely known to induce cracks as graphene is a macroscopic sheet that has to be mechanically maintained while and after the underlying growth catalyst is etched. Polymers are known to protect graphene from cracking and folding at the cost of extensive contamination, highlighting the need for a top phase that can be solidified without the use of polymerization reactions. In this article, we demonstrate that cyclohexane operates similarly as a polymer support, however, without major contamination. Interfacial caging of graphene at a cyclohexane/water interface harvests nonpolar binding interactions between graphene and an organic liquid, still permitting the etching of the growth catalyst from the etchant bottom aqueous phase. Such organic−aqueous interfaces have been used for separating and extracting products of chemical reactions[15,16] and have the potential for in situ graphene functionalization[17,18] and electrochemistry.[19,20]

In this work, the fluidic interface—that is, two immiscible liquids with graphene in between—mechanically and continuously relaxes a graphene monolayer from stresses induced during etching, preventing the formation of the wrinkles always observed in conventional graphene transfers. In addition, the surface tension forces at the cyclohexane−water interface damp down low amplitude vibrations, therefore preventing graphene from cracking, which always occurs when graphene floats on the surface of water without a polymer support. We employ cyclohexane as the organic phase because of several important physical properties: (i) cyclohexane is immiscible with water, (ii) cyclohexane conforms the surface of graphene as copper is etched at room temperature, and most significantly, (iii) cyclohexane solidifies at 7 °C forming a plastic crystal phase, supporting graphene, once the copper is etched. The soft gel-like structure of the plastic crystal phase of cyclohexane (in this paper we only consider the high-temperature solid phase of cyclohexane, stable between −87 °C and melting at 7 °C, see Figure 1a) conforms the surface of graphene preventing mechanical damaging with minimum contamination and handling, as only cooling down from room temperature to 0−7 °C is needed. After transferring to the final substrate, the residues of cyclohexane can be straightforwardly removed at room temperature, while cyclohexane melts and vaporizes.

Additionally, the biphasic design affords intact graphene with high electrical performance while being chemically benign and completely removable from graphene, a key to the transfer of high-quality graphene onto arbitrary substrates for advanced electronics.[21] For the first time, we examined the electric field-effect properties of graphene at the biphasic interface. Preliminary results revealed charge carrier mobility reaching ~3470 $cm^2/(V\,s)$. This key transistor performance parameter is superior to those of the same batch of CVD graphene devices after transferring onto Si/SiO_2 substrate (2180 $cm^2/(V\,s)$) and epoxy substrate (1505 $cm^2/(V\,s)$).

Received: August 19, 2016
Published: November 28, 2016

DOI: 10.1021/acscentsci.6b00236
ACS Cent. Sci. 2016, 2, 904−909

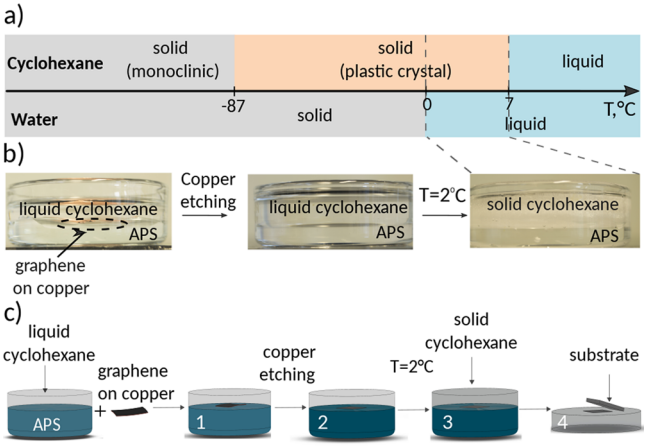

Figure 1. Cyclohexane and water interface for graphene caging and biphasic transfer. (a) Temperature dependence of the state of matter for cyclohexane and water. In the temperature window −87 °C < T < 7 °C cyclohexane forms a plastic crystal phase, whereas water is liquid at the temperatures above 0 °C. (b) Interfacial caging employed in the temperature range T > 0 °C. Biphasic transfer is carried at temperatures between 0 and 7 °C in which cyclohexane is plastic crystal and water is liquid. (c) Illustration depicting the biphasic transfer. Graphene is inserted in the biphasic solution (1), the copper is etched (2), the solution is cooled down to 2 °C until the cyclohexane phase solidifies (3), and the cyclohexane phase with graphene adsorbed is transferred onto a substrate (4). In a last step the sample is kept at 2 °C until the cyclohexane sublimates.

RESULTS AND DISCUSSION

Interfacial Caging of Graphene: The Concept. Water and cyclohexane are immiscible (solubility of cyclohexane in water is 0.006% at 25 °C, solubility of water in cyclohexane is 0.01% at 20 °C) and ammonium persulfate—the copper etchant—is insoluble in cyclohexane, minimizing the interchange of matter between the two phases. Once placed at the meniscus between air and cyclohexane, the graphene/Cu sample sinks to the cyclohexane/water interface and floats there exposing graphene to the cyclohexane phase and copper to the etchant solution (see Figure 1b,c).

When the copper is completely etched, graphene remains floating in between the two phases (Figure 1b). Water and cyclohexane apply pressure on both sides of graphene and serve as a firm but flexible shell conforming the surface of graphene.

Biphasic Transfer: Cool-Down and Stand. After copper is etched, the biphasic oil−water mixture is cooled down to 2 °C (Figure 1c). At 2 °C cyclohexane solidifies and forms a solid mold on the top-side of the graphene surface. The solid cyclohexane phase with adsorbed graphene can be separated from the etchant and rinsed with cold water at 2 °C to remove residues of etchant. The cyclohexane mold is then taken out and placed on the final substrate that has been preliminarily cooled down. The cyclohexane/graphene/substrate stack is then placed in an open container with constant temperature around 0−2 °C (a box with water ice or ventilated fridge in our case). Cyclohexane was then left to sublimate overnight at a temperature ranging from 0 to 4 °C, typically in an ice−water bath or in a ventilated fridge. We used a volume ratio between the two phases of 1:1, typically 10 mL of 0.5 M APS in water and 10 mL of cyclohexane.

An alternative is to directly deposit the substrate on the copper foil covered with graphene at the cyclohexane−water interface. During etching, because of the interfacial tension between water and cyclohexane and also as a result of the Archimedes' upward force acting on the wafer through the cyclohexane, both copper (graphene) and the substrate float at the interface. Next, cyclohexane is solidified and the solid cyclohexane phase with the incrusted substrate with graphene is taken out of the beaker. The fact that graphene was in contact with the substrate from the very start of the transfer prevents the presence of ammonium persulfate residues between graphene and the substrate. The contamination from the other side of graphene can be removed by rinsing the sample with water. The rinsing conditions have to be controlled carefully as it can cause melting of cyclohexane and detachment of graphene.

Crucial to Freeze Cyclohexane. To illustrate the importance of freezing cyclohexane, we performed three control transfer experiments. First, we did not freeze cyclohexane and directly "fished-out", that is, "contact-stamped", the graphene floating at the interface using a silicon wafer. We noticed that the turbulence occurring both in cyclohexane and etchant due to the insertion of the wafer broke the graphene apart. In a second experiment, we placed a wafer on copper/graphene prior etching without freezing the cyclohexane. In both cases, no graphene was transferred to the substrate, which, therefore, indicates the essential role of the solidification of cyclohexane for transferring graphene. In a last experiment we placed a silicon wafer on copper/graphene floating on the etchant without using cyclohexane: again, no graphene was found on the wafer after the transfer.

Integrity and Quality of Graphene Transferred. We compared the graphene properties (continuality, density of cracks, size of wrinkles, density of wrinkles) using interfacial caging with (i) the most commonly used PMMA-based polymer-assisted transfer (Figure 2b),[2,3] (ii) the potentially most "clean" method, which we introduce here as "contact-stamping", where graphene is transferred by pushing down into water a floating graphene flake using a substrate, and (iii) a newly introduced hexane-assisted transfer (see Methods for more details).[14] The PMMA polymer (i.e., poly(methyl methacrylate)) protects and conforms the surface of graphene and therefore allows transferring large and continuous areas of graphene (Figure 2b). Polymer residuals, however, are inevitable, contaminating the surface of the graphene.[11] In contrast, contact-stamping and hexane-assisted transfer methods result in cleaner, but discontinuous, graphene samples with multiple irregularities (foldings, wrinkles, cracks, etc.; see Figure 2c,d). Remarkably, interfacial caging yields large and continuous graphene sheets if transferred onto silicon wafers (Figure 2a) without folding, micrometer-scale wrinkles, and with only a few cracks present in graphene.

Interestingly, the optical micrographs of graphene transferred with interfacial caging and PMMA are similar (Figure 2a versus Figure 2b). Among all the existing transfer methods, interfacial caging and PMMA-assisted method showed similar continuality and the least amounts of cracks (Figure 2a,b). Graphene transferred by contact stamping is less uniform (i.e., very cracked) and has varieties of wrinkles, even more evident on the magnified optical micrographs (Figure 2c, inset). Those wrinkles originate from the moment when graphene floating on the etchant is forced to get in contact with the wafer during stamping. Contact stamped and hexane-based transfers yield similar graphene morphologies: during the scooping out of the graphene from the biphasic system, the graphene brakes into

DOI: 10.1021/acscentsci.6b00236
ACS Cent. Sci. 2016, 2, 904−909

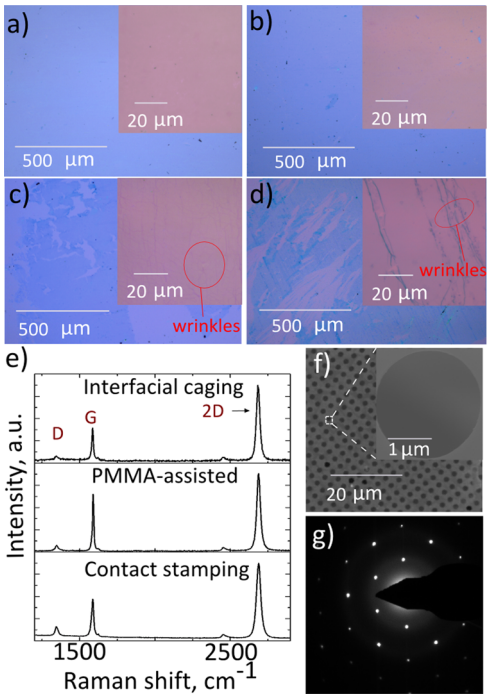

Figure 2. Biphasic transfer contest: comparison with conventional transfer methodologies (PMMA, contact stamping, hexane−water interface). (a) Optical micrograph of graphene transferred using interfacial caging with solidified cyclohexane. (b) Optical micrograph of graphene transferred using the PMMA-assisted method. (c) Optical micrograph of graphene transferred using contact stamping. (d) Optical micrograph of graphene transferred using hexane-assisted method.[14] (e) Raman spectra of graphene transferred onto silicon wafers using interfacial caging, PMMA-assisted and contact stamping. (f) Scanning electron micrograph of graphene transferred to quantifoil electron microscopy grids using the interfacial caging. Inset: zoomed-in view of graphene free-standing on top of a hole on the grid—no contamination, cracks, and foldings are visible. (g) Diffraction pattern of graphene transferred with cyclohexane. TEM was carried out with a 300 kV electron beam focused to a 100 nm probe size at low dose.

smaller pieces and therefore becomes outstandingly wrinkled and cracked (Figure 2c,d).

The Raman spectra of graphene transferred to silicon wafers using interfacial caging, PMMA-assisted method and contact stamping are similar showing the characteristic peaks of monolayer graphene (Figure 2e): a sharp 2D peak (I_{2D}/I_G ratio of 2.4 for interfacial caging, 1.4 for PMMA-assisted, and 2 for contact stamping transfer methods respectively, FWHM of 2D peak around 30 cm^{-1}; see Table 1), that fits one Lorentz function indicating the presence of monolayer graphene,[22] and

Table 1. Raman Characteristics of Graphene Transferred by Interfacial Caging, PMMA-Assisted and Contact Stamping Transfer Methods

	D peak position, cm^{-1}	G peak position, cm^{-1}	2D peak position, cm^{-1}	I_D/I_G	I_{2D}/I_G	FWHM of 2D peak, cm^{-1}
interfacial caging	1343	1587	2686	0.1	2.4	30
PMMA-assisted	1345	1587	2687	0.1	1.4	26
contact stamping	1343	1587	2687	0.2	2	33

a negligible small D peak evidencing almost no defects in the graphene lattice[23] (I_D/I_G ratio of 0.1 for interfacial caging and PMMA-assisted transfer methods and 0.2 for contact stamping, see Table 1). These ratios indicate that the biphasically transferred graphene has a defect density similar to the graphene samples transferred by PMMA-assisted and contact-stamping methods.

Remarkably, if interfacial caging is used to fabricate free-standing graphene devices, a full coverage is achieved in large scale. Figure 2f shows scanning electron micrographs images of the samples transferred using the interfacial caging on holey transmission electron microscope grids. Particularly, graphene membranes are free from wrinkles, tears, and visible contamination (see Figure 2f).

TEM study of graphene transferred to quantifoil grids also showed no traces of cyclohexane. The sample exhibited almost no change in diffraction patterns over 15 min, which indicates that no noticeable contamination took place on graphene surface (Figure 2g). As a comparison, in ref 24 contaminants were shown to get accumulated in the course of 40 s at the area exposed to the electron beam which is seen as amorphization in diffraction patterns.

We further studied graphene transferred by interfacial caging (Figure 3a) using atomic force microscopy (AFM) and

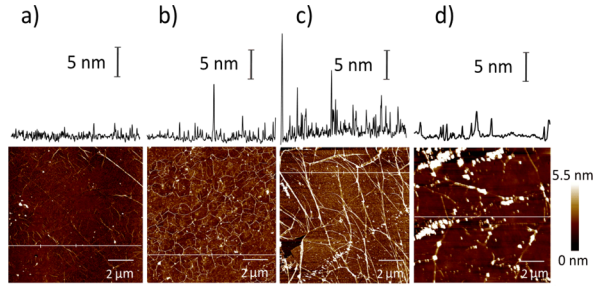

Figure 3. AFM images and height profiles of graphene samples transferred to silicon wafer using interfacial caging and other conventional transfer methods. (a) Interfacial caging method. (b) PMMA-assisted method. (c) Contact stamping method. (d) Hexane-assisted transfer method.[14] The top panel in each image shows the height profile along the line (in white) highlighted in the main image.

compared the results with conventional transfer methods (Figure 3b−d). A typical bad AFM image of graphene transferred to a silicon wafer by PMMA-assisted method has multiple features that correspond to wrinkles, PMMA residues, and dust particles.[8,9,11] PMMA-transferred graphene has multiple topological features (Figure 3b). Those could be interpreted as wrinkles or as polymer residues segregated on the grain boundaries of graphene. The wrinkles are larger for PMMA transferred graphene than for interfacial caging (Figure 3a vs 3b). Contact stamped graphene, as expected, exhibits repetitive patterns of parallel wrinkles (white lines with the length of few micrometers and height up to 10 nm, see Figure 3c), a result in a good agreement with the optical micrographs of the same samples (Figure 2c). The surface of the hexane-transferred graphene also contains wrinkles, but of smaller size with respect to the contact stamped sample, and larger compare to interfacial caging (Figure 3d). The particles that are also seen in AFM images of all three samples can be attributed to dust particles, airborne contaminants, and possibly copper etchant crystals/residuals. Those contaminants are very difficult to

DOI: 10.1021/acscentsci.6b00236
ACS Cent. Sci. 2016, 2, 904−909

avoid when working under atmospheric conditions, and not in a vacuum or in a cleanroom.

Biphasic Electrolyte-Gated Graphene Field-Effect Transistor. In order to confirm that the interfacial transfer procedure affords intact graphene with high electrical performance, we examined the electric field-effect of graphene at the biphasic interface. For device fabrication, while graphene was floating at the organic/water interface, the two source and drain copper electrodes (25 μm Cu) were protected by using PMMA against the etchant, leaving the upper surface for electrical probing (as shown in Figure 4b, top) after etching. As a control,

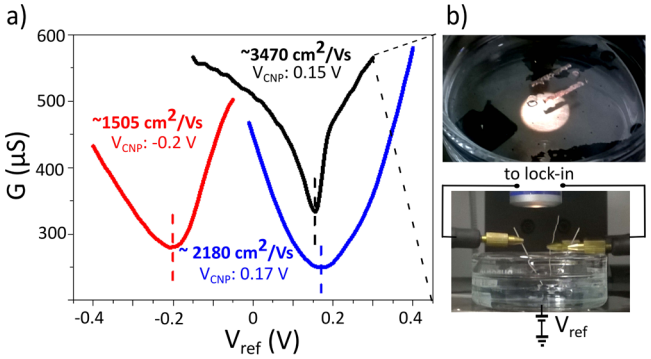

Figure 4. Electrical probing of graphene at the cyclohexane/water interface. (a) The electrolyte gate voltage (V_{ref}) dependent sheet conductance (G) of polymer-free graphene at a cyclohexane/water interface (black), on an epoxy substrate (red) and on a SiO_2/Si substrate (blue). The gate voltage of the charge neutrality point V_{CNP} is 0.15 V for the graphene at the cyclohexane/water interface, compared to −0.2 V on an epoxy substrate and 0.17 V for the graphene on SiO_2/Si. (b) Photographs of the experimental setup used for probing the electronic properties of graphene at the cyclohexane/water interface: top-view (top) and side-view (bottom). As graphene floats at the organic/water interface, its sheet conductance G was measured between the two source and drain copper electrodes (25 μm Cu), which were protected by using PMMA against the etchant, in order to leave the upper copper surface available for needle contact and thus electrical probing.

we fabricated graphene devices on an epoxy substrate and on a SiO_2/Si substrate.[25] Ag/AgCl reference electrodes were used as the electrolyte gate. The transfer curves of these graphene flakes are compared in Figure 4a.

We measured significantly higher carrier mobility on average ~3470 cm^2/(V s) (~1940 cm^2/(V s) for hole, and ~5000 cm^2/(V s) for electron; see Figure 4a) compared to ~1505 cm^2/(V s) (~940 cm^2/(V s) for hole and ~2070 cm^2/(V s) for electron) on the epoxy substrate and ~2180 cm^2/(V s) (~1840 cm^2/(V s) for hole and ~2520 cm^2/(V s) for electron) on the SiO_2/Si substrate. Consequently, the interfacial configuration favors to keep the "as-grown" (i.e., before transfer) electrical properties of graphene. The observed reduction in mobility after transfer onto epoxy or SiO_2/Si (but with electrical properties comparable to CVD graphene after conventional PMMA-assisted transferring onto SiO_2/Si substrates ~100−1400 cm^2/(V s),[26] ~1100 cm^2/(V s)[27]) suggests substrate scattering. High charge carrier mobilities in the case of caged graphene can be ascribed to the absence of polymer contamination. In fact, resist residues can interfere and even prevent surface functionalization, which is an essential step for graphene sensor development. Such a graphene sheet with a clean surface at a biphasic interface is therefore ideal for sensing applications, especially when a flexible and high-performance graphene device is needed. We would like to note here that we did not compare our results with free-standing or h-BN encapsulated graphene transistor devices, which exhibit very high carrier mobilities by removing any possible substrate scattering from, for example, SiO_2/Si substrates. We would also like to mention that depending on the quality of the CVD graphene, the floating graphene devices tend to break if the CVD graphene contains too many defects.

In this article we introduced interfacial caging and compared the benefits of using a biphasic system with the advantages of most used, principal, conventional graphene transfer methodologies. We summarized our results in Table 2.

For polymer-based transfer using PMMA, graphene is supported by a polymer, promoting a stable mold so that further handling and lithography is possible with graphene. The polymer maintains the integrity of graphene, conforms the graphene surface, and prevents graphene from forming large wrinkles. PMMA, however, conforms the catalyst, which is typically rough, hence resulting in wrinkles after transfer. Another drawback of using polymers (PMMA or others) for transfer is the unavoidable presence of polymer residues on graphene, which remains even after several annealing steps. Contact stamping and hexane-assisted transfer result in cleaner but largely cracked and wrinkled graphene.

Interfacial caging allows, on the one hand, to softly support graphene from both its sides, inherently minimizing irregularities such as wrinkles and foldings using the natural difference in surface tension and capillary forces at a water/cyclohexane interface. On the other hand, cyclohexane, contrary to PMMA, is a smaller molecule without a conjugated electron system, i.e., not prone to $\pi-\pi$ stacking on graphene surface (such as benzene for example), which together with its high volatility renders cyclohexane to be very easily removed from graphene. Additionally, interfacial caging and subsequent biphasic transfer only require cooling down a graphene sample without subjecting graphene to harsh treatments. Big areas of graphene can be transferred without inducing defects and multiple big cracks, which was confirmed by Raman spectroscopy, optical, atomic force microscopy, and scanning electron microscopy.

While interfacial caging is an appealing method for industrial applications, the technique opens new modalities for fundamental studies of floating graphene. For lithographic purposes, however, the method may be less appealing unless a

Table 2. Comparative Analysis of Graphene Samples Transferred with Interfacial Caging, PMMA-Assisted Method, Contact Stamping, and Hexane-Assisted Method

	interfacial caging method	PMMA-assisted method	contact stamping	hexane-assisted method
continuality	full coverage of the wafer	full coverage of the wafer	partial coverage of the wafer	partial coverage of the wafer
density of cracks	low	low	high	high
size of wrinkles	2−3 nm high, 0.5−2 μm long	2−15 nm high, up to 10 μm long	>15 nm high, >10 μm long	2−15 nm high, up to 10 μm long
density of wrinkles	low	high	high	medium

DOI: 10.1021/acscentsci.6b00236
ACS Cent. Sci. 2016, 2, 904−909

physical (nonsticky) mask is used for patterning. For the first time, our interfacial approach enables electrical measurement of electrolyte-gated graphene field-effect transistors with improved electrical performance for graphene caged at a cyclohexane/water interface. The remarkably higher carrier mobility of a floating graphene flake compared to that of its counterpart after transfer onto either epoxy or SiO_2/Si substrates suggests that the intrinsic electrical properties of graphene are largely retained presumably thanks to minimal contaminations. Such high-performance, flexible graphene transistors in a floating configuration can be readily used for in situ sensing liquid/liquid interfaces.

METHODS

Growth and Transferring of Graphene. Copper foil with the thickness of 25 μm was annealed at 1035 °C, and the monolayer graphene films were grown using chemical vapor deposition.[28] After the CVD synthesis, the graphene grown on the backside of the copper foil was removed by using oxygen plasma. After etching the graphene at the backside of the copper foil, we placed the piece at the interface of a biphasic mixture of cyclohexane and water supplemented with ammonium persulfate (i.e., the copper etchant). For transferring the graphene onto substrates with the interfacial caging method, we followed the approaches described in the Results and Discussion section of this article. All samples were rinsed with water and ethanol after the transfer. For the PMMA-assisted method, we reproduced the protocol from ref 3. For the contact stamping method, a wafer was directly placed on graphene floating on the etchant, transferred, and rinsed with water; alternatively, the etchant is replaced by pure water prior stamping. For the hexane-assisted transfer method, we reproduced the protocol from ref 14 by placing a wafer beneath graphene (in the etchant) and fishing from below the graphene with hexane as the top phase. In all four transfer methods, we used a 0.5 M solution of $(NH_4)_2S_2O_8$ as a copper etchant.

Characterization. *Raman Spectroscopy.* Micro-Raman spectroscopy was performed with a commercial inVia model from Renishaw spectrometer setup with a dual-axis XY piezo stage. A laser with 532 nm excitation wavelength was used. The grating has 600 lines/mm. Raman spectra are recorded in air with a 100× objective. We limited the laser power to below 2 mW to prevent any laser-induced heating of the samples.

AFM. All AFM experiments with graphene on silicon wafers were carried out on a Multimode Bruker (ex-DI) Nanoscope V. The experiments were performed using a silicon 254 probe (AC160TS, Asylum Research) with 300 kHz nominal resonance frequency. The images were scanned in an intermittent contact mode at room temperature with 512 × 512 pixels. All the samples have been annealed at 400 °C prior to the imaging.

SEM. SEM of graphene transferred to TEM quantifoil grids was performed with FEI NANOSEM 200 at 10 kV. For the measurements, graphene samples were transferred to quantifoil grids using the interfacial caging method.

Electrical Measurements. To evaluate the quality of the transferred graphene in a large area, in this study we fabricated graphene transistors with a channel length of several millimeters. As the contact resistance between our graphene and metal electrodes (both are of large area) is negligible, we applied two-point source-drain measurements, and all the results were normalized by using the length/width ratio of the graphene transistors to obtain their field-effect mobility numbers. The transistor characteristics of the electrolyte-gated graphene field-effect transistor devices with different geometry were tested using a homemade setup. A SR830 DSP lock-in amplifier with narrow filters was used to recover a weak signal from a noisy background. The electrolyte gate voltage V_{ref} (up to ±0.4 V) was applied to a Ag/AgCl reference electrode immersed in the electrolyte.

For the electrical probing of graphene samples floating at the biphasic interface, the etchant solution was replaced with 0.1 M solution of KCl. During the replacement of the etchant solution, the entire mixture was cooled down to freeze the cyclohexane phase in order to avoid the effect of vibrations on the integrity of the graphene sheet.

AUTHOR INFORMATION

Corresponding Author

*E-mail: g.f.schneider@chem.leidenuniv.nl.

ORCID

Liubov A. Belyaeva: 0000-0001-8958-9891

Notes

The authors declare no competing financial interest.

ACKNOWLEDGMENTS

This research was supported by the European Research Council under the European Union's Seventh Framework Programme (FP/2007-2013)/ERC Grant Agreement No. 335879 project acronym "Biographene", The Netherlands Organization for Scientific Research (NWO-VIDI 723.013.007). W.F. gratefully acknowledges financial support by The Netherlands Organization for Scientific Research (NWO-VENI 722.014.004) and the Swiss National Science Foundation (SNSF P300P2_154557). We thank Jan Aarts, Marc Koper, Alexander Kros, and Sense Jan de Molen for helpful discussions. We thank Henny Zandbergen for discussions and his support on diffraction studies. AFM measurements were performed in the AFM Lab of the Leiden Institute of Physics.

REFERENCES

(1) Novoselov, K. S.; Geim, A. K.; Morozov, S. V.; Jiang, D.; Zhang, Y.; Dubonos, S. V.; Grigorieva, I. V.; Firsov, A. A. Atomically Thin Carbon Films. *Science* **2004**, *306*, 666−669.

(2) Li, X.; Zhu, Y.; Cai, W.; Borysiak, M.; Han, B.; Chen, D.; Piner, R. D.; Colombo, L.; Ruoff, R. S. Transfer of Large-Area Graphene Films for High-Performance Transparent Conductive Electrodes. *Nano Lett.* **2009**, *9*, 4359−4363.

(3) Suk, J. W.; Kitt, A.; Magnuson, C. W.; Hao, Y.; Ahmed, S.; An, J.; Swan, A. K.; Goldberg, B. B.; Ruoff, R. S. Transfer of CVD-Grown Monolayer Graphene onto Arbitrary Substrates. *ACS Nano* **2011**, *5*, 6916−6924.

(4) Wood, J. D.; Doidge, G. P.; Carrion, E. a; Koepke, J. C.; Kaitz, J. a; Datye, I.; Behnam, A.; Hewaparakrama, J.; Aruin, B.; Chen, Y.; et al. Annealing Free, Clean Graphene Transfer Using Alternative Polymer Scaffolds. *Nanotechnology* **2015**, *26*, 055302.

(5) Gao, L.; Ni, G.-X.; Liu, Y.; Liu, B.; Castro Neto, A. H.; Loh, K. P. Face-to-Face Transfer of Wafer-Scale Graphene Films. *Nature* **2013**, *505*, 190−194.

(6) Feng, Y.; Huang, S.; Kang, K.; Duan, X. Preparation and Characterization of Graphene and Few-Layer Graphene. *New Carbon Mater.* **2011**, *26*, 26−30.

(7) Su, Y.; Han, H.-L.; Cai, Q.; Wu, Q.; Xie, M.; Chen, D.; Geng, B.; Zhang, Y.; Wang, F.; Shen, Y. R.; et al. Polymer Adsorption on Graphite and CVD Graphene Surfaces Studied by Surface-Specific Vibrational Spectroscopy. *Nano Lett.* **2015**, *15*, 6501−6505.

DOI: 10.1021/acscentsci.6b00236
ACS Cent. Sci. 2016, 2, 904−909

(8) Han, Y.; Zhang, L.; Zhang, X.; Ruan, K.; Cui, L.; Wang, Y.; Liao, L.; Wang, Z.; Jie, J. Clean Surface Transfer of Graphene Films via an Effective Sandwich Method for Organic Light-Emitting Diode Applications. *J. Mater. Chem. C* **2014**, *2*, 201−207.
(9) Hallam, T.; Berner, N. C.; Yim, C.; Duesberg, G. S. Strain, Bubbles, Dirt, and Folds: A Study of Graphene Polymer-Assisted Transfer. *Adv. Mater. Interfaces* **2014**, *1*, 1400115.
(10) Pirkle, a.; Chan, J.; Venugopal, a.; Hinojos, D.; Magnuson, C. W.; McDonnell, S.; Colombo, L.; Vogel, E. M.; Ruoff, R. S.; Wallace, R. M. The Effect of Chemical Residues on the Physical and Electrical Properties of Chemical Vapor Deposited Graphene Transferred to SiO2. *Appl. Phys. Lett.* **2011**, *99*, 122108.
(11) Kumar, K.; Kim, Y.-S.; Yang, E.-H. The Influence of Thermal Annealing to Remove Polymeric Residue on the Electronic Doping and Morphological Characteristics of Graphene. *Carbon* **2013**, *65*, 35−45.
(12) Lin, W.-H.; et al. A Direct and Polymer-Free Method for Transferring Graphene Grown by Chemical Vapor Deposition to Any Substrate. *ACS Nano* **2014**, *8*, 1784−1791.
(13) Algara-Siller, G.; Lehtinen, O.; Wang, F. C.; Nair, R. R.; Kaiser, U.; Wu, H. a; Geim, a K.; Grigorieva, I. V. Square Ice in Graphene Nanocapillaries. *Nature* **2015**, *519*, 443−445.
(14) Zhang, G.; Güell, A. G.; Kirkman, P. M.; Lazenby, R. a; Miller, T. S.; Unwin, P. R. Versatile Polymer-Free Graphene Transfer Method and Applications. *ACS Appl. Mater. Interfaces* **2016**, *8*, 8008−8016.
(15) Treybal, R. E. Liquid Extraction. *Ind. Eng. Chem.* **1951**, *94*, 91−99.
(16) Joshi, M. D.; Anderson, J. L. Recent Advances of Ionic Liquids in Separation Science and Mass Spectrometry. *RSC Adv.* **2012**, *2*, 5470−5484.
(17) Toth, P. S.; Ramasse, Q. M.; Velický, M.; Dryfe, R. a. W. Functionalization of Graphene at the Organic/water Interface. *Chem. Sci.* **2015**, *6*, 1316−1323.
(18) Toth, P. S.; Velický, M.; Ramasse, Q. M.; Kepaptsoglou, D. M.; Dryfe, R. a. W. Symmetric and Asymmetric Decoration of Graphene: Bimetal-Graphene Sandwiches. *Adv. Funct. Mater.* **2015**, *25*, 2899−2909.
(19) Rodgers, A. N. J.; Dryfe, R. a. W. Oxygen Reduction at the Liquid-Liquid Interface: Bipolar Electrochemistry through Adsorbed Graphene Layers. *ChemElectroChem* **2016**, *3*, 472−479.
(20) Feng, Y.; Chen, K. Dry Transfer of Chemical-Vapor-Deposition-Grown Graphene onto Liquid-Sensitive Surfaces for Tunnel Junction Applications. *Nanotechnology* **2015**, *26*, 035302.
(21) Banszerus, L.; Schmitz, M.; Engels, S.; Dauber, J.; Oellers, M.; Haupt, F.; Watanabe, K.; Taniguchi, T.; Beschoten, B.; Stampfer, C. Ultrahigh-Mobility Graphene Devices from Chemical Vapor Deposition on Reusable Copper. *Sci. Adv.* **2015**, *1*, 1−6.
(22) Ferrari, A. C.; Basko, D. M. Raman Spectroscopy as a Versatile Tool for Studying the Properties of Graphene. *Nat. Nanotechnol.* **2013**, *8*, 235−246.
(23) Ferrari, A. C.; Basko, D. M. Raman Spectroscopy as a Versatile Tool for Studying the Properties of Graphene. *Nat. Nanotechnol.* **2013**, *8*, 235−246.
(24) Schneider, G. F.; Xu, Q.; Hage, S.; Luik, S.; Spoor, J. N. H.; Malladi, S.; Zandbergen, H.; Dekker, C. Tailoring the Hydrophobicity of Graphene for Its Use as Nanopores for DNA Translocation. *Nat. Commun.* **2013**, *4*, 2619−2626.
(25) Fu, W.; Nef, C.; Tarasov, a; Wipf, M.; Stoop, R.; Knopfmacher, O.; Weiss, M.; Calame, M.; Schönenberger, C. High Mobility Graphene Ion-Sensitive Field-Effect Transistors by Noncovalent Functionalization. *Nanoscale* **2013**, *5*, 12104−12110.
(26) Liang, X.; Sperling, B. A.; Calizo, I.; Cheng, G.; Hacker, C. A.; Zhang, Q.; Obeng, Y.; Yan, K.; Peng, H.; Li, Q.; et al. Toward Clean and Crackless Transfer of Graphene. *ACS Nano* **2011**, *5*, 9144−9153.
(27) Song, H. S.; Li, S. L.; Miyazaki, H.; Sato, S.; Hayashi, K.; Yamada, A.; Yokoyama, N.; Tsukagoshi, K. Origin of the Relatively Low Transport Mobility of Graphene Grown through Chemical Vapor Deposition. *Sci. Rep.* **2012**, *2*, 337.
(28) Pierson, H. O. *Handbook of Chemical Vapor Deposition (CVD)*; Noyes Publications/William Andrew Publishing, LLC: Norwich, New York, U.S.A, 1999.

DOI: 10.1021/acscentsci.6b00236
ACS Cent. Sci. 2016, 2, 904−909